UDK: 533.6.071:336.763,533.695.7:548.121,622.428.8
COSATI: 01-01
doi: 10.5937/str2102019D

Wind Tunnel Verification of Base-Bleed Effects on Aerodynamic Characteristics of an Axi-Symmetric Projectile

Dijana Damljanović [1)]
Goran Ocokoljić [1)]
Miodrag Lisov [1)]
Danilo Đurđevac [1)]

Experimental verification of base-bleed effects on aerodynamic characteristics for the supersonic flight stages was requested during the development of an axi-symmetric projectile. The experimental setup for testing base-bleed configurations of the projectile was designed, built and tested in the T-38 trisonic blowdown wind tunnel of the Military Technical Institute (VTI), Belgrade. Gas-generator was formed from a simple chamber with a single manifold pneumatically connected to a high-pressure air supply. Wind tunnel tests comprised measurement of aerodynamic forces and moments of the projectile with active base-bleed. Flow visualization was performed using the Schlieren method. It was of interest to verify the base drag reduction in the wind tunnel tests and to compare it with numerical predictions. In addition, the experience gained during these tests has been found to be helpful in the design of the future similar wind tunnel setups

Key words: **wind tunnel, projectile, gas generator, base-bleed, aerodynamic characteristics, base drag.**

Introduction

DURING a flight of a projectile a low pressure area exists behind the base, producing the so called base drag force, which influences the velocity of the projectile.

For types of aerodynamic bodies, such as artillery proje-ctiles, the drag in the base region has a significant contribution to the total drag. It was found that for aerodynamically optimized extended range projectiles (such as 122 mm HEER-BB) the base drag is responsible for up to 75% of the total drag in the high-subsonic speed range (Mach 0.9) and about 50%-55% for Mach numbers higher than 1.2. In order to achieve a long range, a high initial velocity of the projectile is necessary (Mach 2.1 for 122 mm HEER-BB projectile).

It is known that the drag force in supersonics is signifi-cantly larger than in subsonics and it increases with square velocity. Also, it should be noted that, after the launch, the projectile flies through the denser atmospheric layers, which additionally increase the drag force. So, reducing the base drag is very efficient way to reduce the total drag of the projectile.

Considerable effort has been made to find suitable techniques for obtaining a low base drag. Two methods of drag reduction are typically used. The first is to optimize the shape of the projectile, using a boattail afterbody which reduces the base surface area exposed to the afterbody expansion which increases the base pressure. The second method consists of increasing the pressure behind the projectile by base burning. This can be accomplished with injection of a low velocity fluid in the recirculation region directly behind the base.

The base drag can be reduced or, theoretically, even eliminated by flowing out a stream of hot gas from the base of the projectile, a technique which is known as base-bleed. Numerical simulations [1] and test range results showed the reduction of total drag of about 35% in the supersonic regime for artillery projectiles with active base-bleed.

During the development of an axi-symmetric projectile a designer was interested in experimental verification of operational parameters of the base-bleed unit and its effects on aerodynamic characteristics of the projectile. Therefore, the experimental setup for testing base-bleed configurations of the projectile in the T-38 trisonic blowdown wind tunnel of the Military Technical Institute (VTI), Belgrade, has been designed [2]. The design concept was based on the experience obtained in the tests of models with lateral jets performed in the VTI large subsonic wind tunnel facility [3]-[7].

The T-38 wind tunnel test comprised measurement of aerodynamic forces and moments of the projectile, as well as base pressure, with simulation of the base-bleed of combustion products. The designer was interested in a contribution of the base-bleed on flight characteristics of the projectile in the Mach number range from 1 to 2.

The experimental results were used in the optimization of the base-bleed unit during the development phase of the projectile. Here, the experience and some discussion on wind tunnel test results based on previous work concernig this problematic [3]-[8] has been given.

Wind tunnel model

In accordance with the request for experimental verification of the base-bleed effects of the combustion products on aerodynamic characteristics of the projectile, a wind tunnel model was designed and produced, Fig.1.

The model had to be designed and produced in a way to adjust a base-bleed configuration to the wind tunnel model

[1)] Military Technical Institute (VTI), Ratka Resanovića 1, 11132 Belgrade, SERBIA
Correspondence to: Dijana Damljanović, e-mail: didamlj@gmail.com

support system and to enable the model mounting on the wind tunnel balance.

For investigation of the base-bleed efects, a gas-generator was formed from a simple chamber with a single manifold pneumatically connected to a high pressure air supply existing in the wind tunnel, Figures 1 and 2. During the test the chamber was filled up with pressurized air and simulation of the base-bleed was achieved by flowing out through the 35 mm diameter exit nozzle.

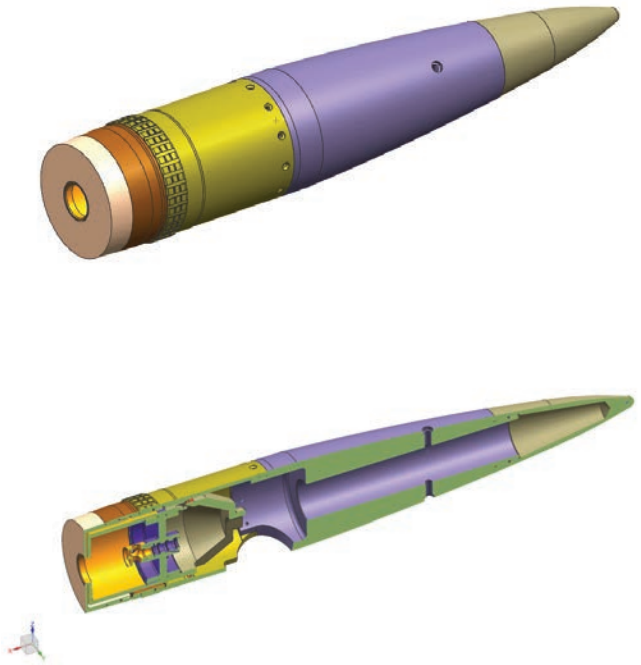

Figure 1. CAD model of the wind tunnel model

Wind tunnel balance for the measurements of aerodynamic forces and moments was the six-component 2in Able Mk XVIII. The Able balance and the chamber were mounted on the 71° bent sting using an adaptor, Fig.2.

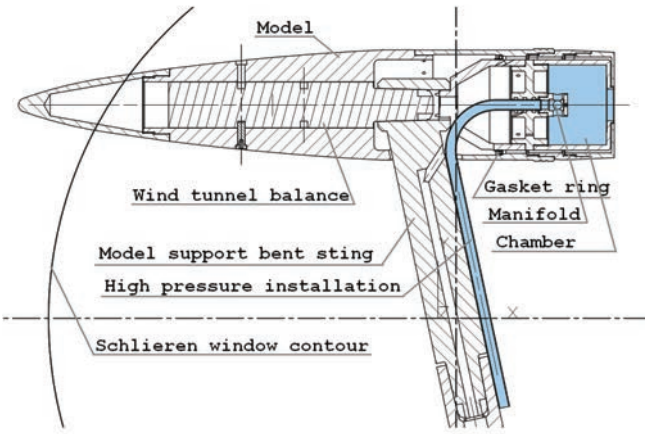

Figure 2. The model's chamber for the base-bleed simulation with the high pressure air installation plunged in

The chamber was isolated from the model using an elastic gasket ring in order to minimize influences on the measurement of the model loads. The complete model mounted on the 71° model support bent sting is shown in Figures 3 and 4. For the model support pitch angle zero, the model was in the –7° angle of attack position [9]-[11].

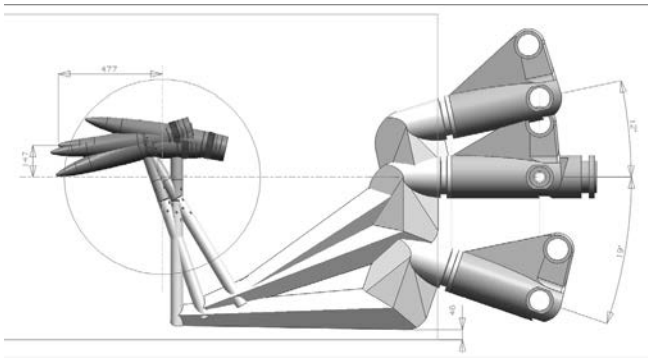

Figure 3. CAD model of the projectile on the 71° bent sting moved to the –12°, 0°, +19° pitch angle positions

Model of the projectile mounted on the 71° bent sting in the T-38 wind tunnel test section and moved to the +19° pitch angle position is presented in Fig.4.

Figure 4. Model of the projectile on the 71° bent sting in the T-38 wind tunnel test section.

Test facility

The T-38 test facility is a blowdown-type pressurized wind tunnel [12] with a 1.5 m square test section, Fig.5. For subsonic and supersonic tests, the test section is with solid walls, while for transonic tests, a section with porous walls is inserted in the configuration. The porosity of walls may vary between 1.5% and 8%, depending on the Mach number, so as to achieve the best flow quality.

Mach number in the range 0.2 to 4.0 can be achieved in the test section, with the Reynolds numbers up to 110 million per meter. In the subsonic configuration, the Mach number is set by sidewall flaps in the tunnel diffuser. In the supersonic configuration, the Mach number is set by the flexible nozzle contour, while in transonic configuration the Mach number is set both by the sidewall flaps and the flexible nozzle, and actively regulated by the blow-off system. The Mach number can be set and regulated to within 0.3% of the nominal value.

Stagnation pressure in the test section can be maintained between 1.1 bar and 15 bar, depending on the Mach number, and regulated to 0.1% of nominal value. Run times are in the range 6s to 60s, depending on the Mach number and stagnation pressure.

The model is supported in the test section by a tail sting mounted on a pitch-and-roll mechanism by which desired aerodynamic angles can be achieved. The facility supports both step-by-step model movement and continuous move-

ment of the model (sweep) during measurements. Positioning accuracy is 0.05° in both pitch and roll.

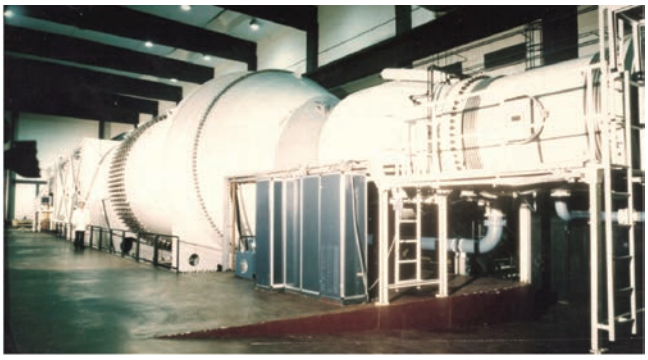

Figure 5. The T-38 test facility in VTI, Belgrade

The high-pressure air supply

The T-38 auxiliary high-pressure air supply that was used for gas-generator simulation consists of two 270 bar Bauer compressors, 200 bar high-pressure tubing, tanks and valves.

High-pressure installation is pneumatically conected to the T-38 test facility. The installation is charged up to 200 bar. Humidity separation is done on the compressors themselves and, additionally, in air preparation. Pressurized air after the fourth stage of the compressor is run through an air dryer. After the preparation the air is stored in 14 tanks with 10 m^3 of total volume.

Mass flow rate

It was necessary to find a convenient formula for the mass flow in terms of Mach number, stagnation pressure and stagnation temperature by means of the isentropic law. Starting with the equation of continuity, the following rearrangements have been made:

$$\dot{m} = \rho_{st} \cdot v \cdot A \,. \tag{1}$$

Velocity can be given as a function of the pressure ratio:

$$v = \sqrt{\frac{2 \cdot k}{k-1} \cdot \frac{p_0}{\rho_0} \cdot \left[1 - \left(\frac{p_{st}}{p_0} \right)^{\frac{k-1}{k}} \right]} \,. \tag{2}$$

Static density is computed as:

$$\rho_{st} = \rho_0 \cdot \left(\frac{p_{st}}{p_0} \right)^{\frac{1}{k}} \,. \tag{3}$$

Based on relations (1-3) mass flow can be presented as the function of the pressure ratio:

$$\dot{m} = A \cdot \sqrt{\frac{2 \cdot k}{k-1} \cdot p_0 \cdot \rho_0 \cdot \left[\left(\frac{p_{st}}{p_0} \right)^{\frac{2}{k}} - \left(\frac{p_{st}}{p_0} \right)^{\frac{k+1}{k}} \right]} \,. \tag{4}$$

If density is computed based on the relation of the ideal gas as:

$$\rho_0 = \frac{p_0}{R \cdot T_0} \,, \tag{5}$$

mass flow can be defined based on p_0 – total (stagnation) pressure, p_s – static pressure and T_0 – total (stagnation) temperature, where the A – cross-section area , k – ratio od specific heats and R – gas constant.

Measurement setup

Setup for the mass flow determination was formed based on measured pressures and temperature according to (4) and (5), where the parameters p_{0gen} – total (stagnation) pressure, p_{sgent} – static pressure and T_{0gen} – total (stagnation) temperature were measured in the high-pressure instalation; cross-section area on the exit of the high-pressure 10 mm tube $A = 7.85 \times 10^{-5}$ m^2, ratio od specific heats k = 1.4 and gas constant R = 287 Nm/kgK.

Transducer for stagnation temperature measurement was formed at the end of the pneumatic manifold in the simulated gas-generator as a Wheatstone bridge with temperature-sensitive strain gauges, Fig.6, and calibrated prior to test in a thermal chamber in the –20°C to +27°C range [2].

Figure 6. Stagnation temperature strain-gauge transducer

Total p_{0gen} and static p_{stgen} pressures in the pipe were measured using two absolute pressure Teledyne Taber 2210 transducers of the 100 bar range placed inside the model support system. Both transducers were calibrated up to 20 bar. Pressure taps and temperature station with traced pneumatic and electrical lines are shown in Fig.7.

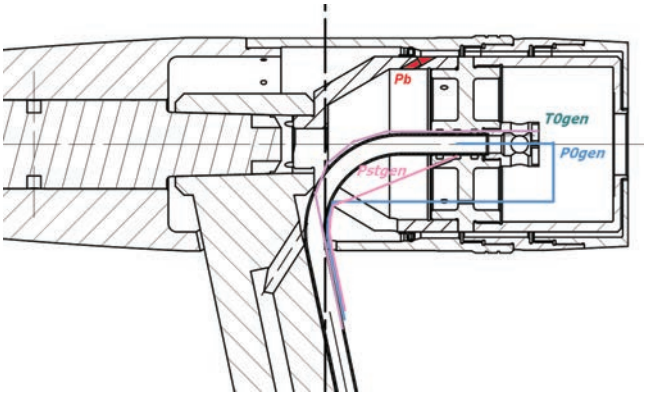

Figure 7. Measurement taps with traced pneumatic and electrical lines

The 1.6 mm dia. metal pipe for total p_{0gen} pressure measurement was adapted and plunged through the manifold inside the 12 mm dia. metal pipe of the high pressure installation, Fig.8. Static p_{stgen} pressure was measured on the wall of the 12 mm dia. metal pipe, Fig.7.

Base pressure p_b on the model was measured by a Druck PDCR42 piezoresistive differential pressure transducer. The active side of this transducer was connected to an orifice that was formed on the chamber wall, Fig.7, for base pressure measurement. The reference side of the transducer was

connected to the tubing leading from the static pressure port on the wall of the test section. The range of this transducer was 0.35 bar, with 0.05% F.S. nonlinearity and hysteresis.

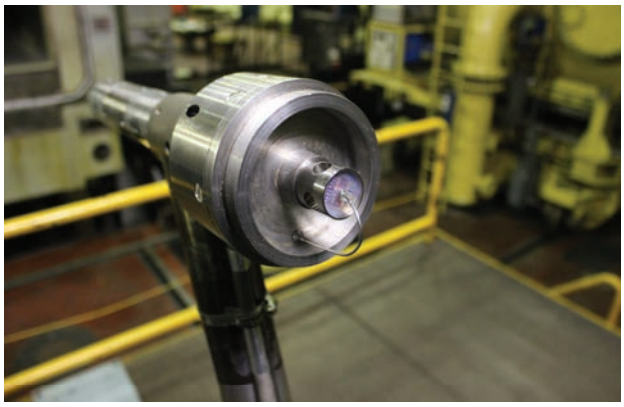

Figure 8. Pressurized-air manifold with formed temperature transducer

Results and discussion

The wind tunnel tests were performed by varying the pressures from high-pressure air supply so the different mass flow rates were achieved. Numerically obtained base-bleed parameters, given by the designer of the projectile [13], were the only input in the experimental setup design. The wind tunnel tests of the projectile were performed in the Mach number range from 1.5 to 2.

Numerical simulations

Drag force coefficients were numerically predicted for the Mach number from 0.99 to 2.1 at different flight regimes, [13]. Numerical steady state simulations of the base-bleed effects on aerodynamic characteristics of the projectile with two turbulences model were done for each Mach number. A turbulence k-ε realizable model was selected as the best agreement with semi-empirical predictions were found.

Nine cases of elements trajectory of the projectile were investigated and for every case the point on trajectory, velocity of projectile, air ambient pressure and temperature were chosen [13]. The first case corresponds to a zero altitude at the beginning of the base-bleed operation. When the base-bleed starts to operate, the projectile velocity is 715 m/s and mass flow rate of combustion products is 0.05 kg/s. For the other cases, projectile velocities, air pressure, mass flow rates of combustion products are shown in Table 1. The drag force coefficients C_D with and without using the base-bleed unit were numerically estimated [13].

Table 1. Elements of the projectile trajectory in the shooting at maximum range during the base-bleed operation, source [13]

Flight time (s)	Altitude (m)	Velocity of projectile (m/s)	Mach number	Air ambient pressure (mbar)	Mass flow rate (10^{-3} kg/s)
0.0	0.0	715.0	2.10	1013.2	50.0
2.54	1237.1	633.9	1.89	873.2	45.6
5.18	2352.5	569.7	1.72	760.8	40.9
9.72	3954.7	484.4	1.49	620.7	33.0
14.53	5278.1	411.5	1.29	520.4	24.6
18.06	6033.3	366.5	1.16	469.7	18.4
21.90	6668.4	326.3	1.04	430.1	11.7
22.68	6774.4	319.5	1.02	423.8	10.3
24.00	6934.5	309.9	0.99	414.4	8.0

Wind tunnel test results

Wind tunnel test results are given in Tables 2-4 for the Mach number 1.5, 1.75 and 2.0. The tables contain values of the regulated entry pressure that was varied to achieve different mass flow rates in the chamber, which are given in the second columns. Base drag coefficient C_{xb} of the model at the zero angle of attack that corresponds to a different mass flow rates is given in the third columns of the Tables 2-4.

Base drag coefficient C_{xb} was calculated based on the base pressure measurement as:

$$C_{xb} = -C_{pb} \cdot \frac{S_b}{S_{ref}} \tag{6}$$

where S_{ref} is the model reference area and S_b is the model base area. Base pressure coefficient C_{pb} was calculated as:

$$C_{pb} = \frac{p_b - p_{st}}{q} \tag{7}$$

where p_b is the base pressure, p_{st} is the static pressure and q is dynamic pressure in the wind tunnel test section.

Table 2. Test results, Mach 1.50

Test Section Parameters: Mach number 1.50 p_{st}=0.643bar, T_0=286K, T_{st}=198.7K		
Regulated entry pressure, bar	Mass flow rate,kg/s	C_{xb}
0	0.00	0.2183
10	0.024	0.2083
20	0.031	0.2079
30	0.054	0.2072
40	0.074	0.2068
50	0.097	0.2093
60	0.123	0.2145
80	0.168	0.2293

Table 3. Test results, Mach 1.75

Test Section Parameters: Mach number 1.75, p_{st}=0.482bar, T_0=286.2K, T_{st}=178.8K		
Regulated entry pressure, bar	Mass flow rate,kg/s	C_{xb}
0	0.00	0.1985
5	0.036	0.1821
10	0.030	0.1822
20	0.034	0.1827
30	0.055	0.1839
40	0.079	0.1863
50	0.100	0.1912

Table 4. Test results, Mach 2.00

Test Section Parameters: Mach number 2.00, p_{st}=0.334bar, T_0=286.9K, T_{st}=161.3K		
Regulated entry pressure, bar	Mass flow rate,kg/s	C_{xb}
0	0.00	0.1811
10	0.021	0.1706
20	0.032	0.1705
30	0.055	0.1736
40	0.079	0.1803
50	0.097	0.1848

The base drag coefficient at the zero angle of attack and corresponding mass flow rates achieved in the chamber in the the wind tunnel tests are presented in Fig.9.

Mass flow rate in the model chamber depends on the static pressure and the static temperature in the wind tunnel test section. The static parameters in the real flight and the wind tunnel test section are NOT the same. So, the model chamber mass flow rates had to be scaled to obtain corresponding real flight mass flow rates.

Scale factors (given in Table 5) for transferring the model chamber mass flow data to the real flight data were calculated based on the wind tunnel and the real flight static parameters (given in Tables 4-6 and Table 3).

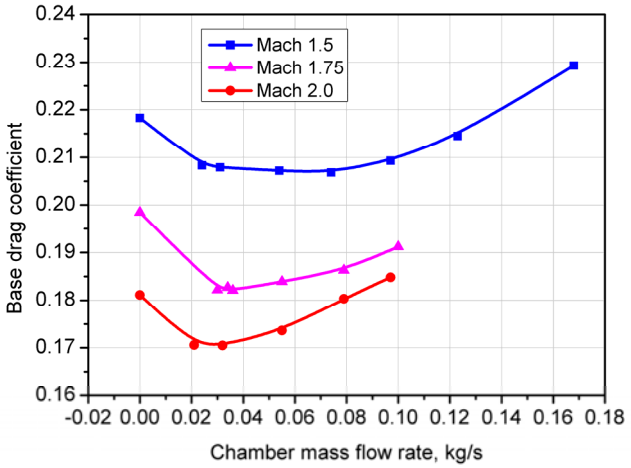

Figure 9. Base drag coefficients at the zero angle of attack vs. chamber mass flow achieved in the wind tunnel

Table 5. Scale factors for transferring the model chamber mass flow data to the real flight data

Mach	Real flight		Wind tunnel	Scale factor, (p_{st}/T_{st} fligth/ p_{st}/T_{st} tunnel)
	Altitude, m	p_{st}/T_{st}, mbar/K	p_{st}/T_{st}, mbar/K	
1.49	3954	2.363	3.236	0.730
1.72	2352	2.79	2.696	1.035
2.0	<1000	3.32	2.071	1.603
$\dot{m}_{RealFlight} = SF_{Tunnel}^{Flight} \times \dot{m}_{WindTunnel}$				

Obtained mass flow data were scaled for the real flight using the scale factors and calculated values are given in the form of a graph in Fig.10.

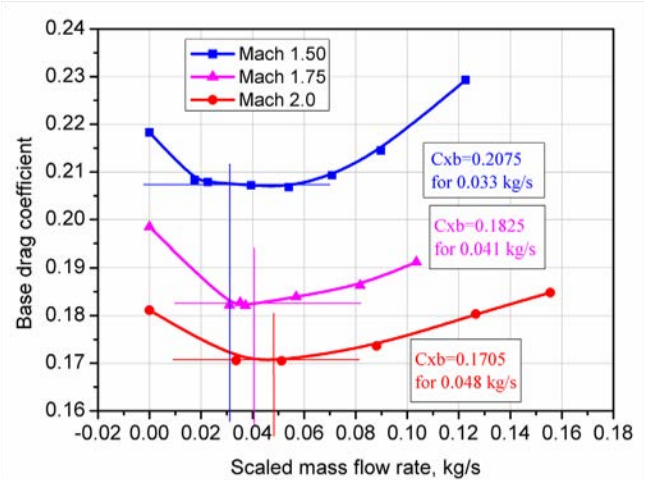

Figure 10. Base drag coefficient at the zero angle of attack vs. mass flow scaled for the real flight

It was observed that the base drag curve for different mass flow rates has a minimum on certain mass flow rate. It was also found that the mass flow rates for minimum base drag coefficient correspond very good with desired values given by the designer of the projectile, see Table 1. The base drag coefficients at the zero angle of attack for given mass flow rates were determined and used in the discussion.

Discussion

The numerically obtained drag reduction using the gas generator unit for all flight stages of the projectile, given in [13], showed that the average reduction is within the range of 4% to 12% for all flight stages, Fig.11. The highest drag reduction was numerically obtained for the supersonic flight stages, from Mach 2.1 up to Mach 1.5 (about 11%) [13].

It was of interest to obtain the base-bleed effects in the wind tunnel tests which corespond to the supersonic flight stages of the projectile. The base drag force coefficients for the given mass flow rates were determined, see Fig.10. It was found that the base drag reduction using the active base-bleed in the wind tunnel tests is about 5% to 8% (Table 6). Numerically and experimentally obtained base-bleed effects on the drag reduction of the projectile are presented in Fig.11. It should be noted that the graph in Fig.11 presents total drag force coeffcients that were numerically calculated and base drag force coefficent measured in the wind tunnel tests. It can be concluded that the character of the drag recuction has been confirmed, although the total drag reduction in percentages are not the same.

Numerical estimates given in [1] showed that drag reduction of this type of projectile in the supersonics flight regimes is about 35%. Firing range tests for the real projectile using base-bleed showed the significant drag reduction (about 40%) during initial flight stages, at supersonic Mach numbers, when the mass flow rate of the combustion products are the highest.

However, the wind tunnel test data showed the dependancy of the base drag on mass flow rates and the designer found them to be very useful in the optimization of operational parameters of the base-bleed unit.

Table 6. Base drag reduction using the active base-bleed

Mach number	Base drag coef. (base-bleed inactive)	Base drag coef. (base-bleed active)	Mass flow rate, kg/s	Base drag reduction, %
2.00	0.1811	0.1705	0.048	~6
1.75	0.1985	0.1825	0.041	~8
1.50	0.2183	0.2075	0.033	~5

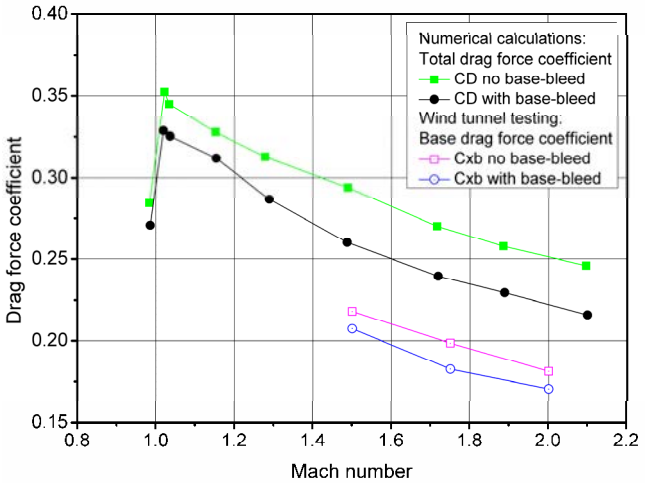

Figure 11. Numerically (regenerated from [13]) and experimentally (T-38 wind tunnel tests) obtained base-bleed effects on the drag reduction

Flow visualization

Flow visualization was performed using the Schlieren method, [14]. Flow patterns around the model at Mach numbers 1.5 and 2.0 in the T-38 wind tunnel are illustrated by snapshots from video recordings of the Schlieren visualizations shown in Fig.12 and Fig.13.

Density gradients positive in the downstream direction are represented in blue colour while the density gradients negative in the same direction are represented in red. In the darkened areas present in the images the gradients exceeded the set sensitivity range of the Schlieren system and the effect was exacerbated by the less-than-perfect collimation of the system optics. The Schlieren technique shows the density gradients (actually, gradients of the refractive index) integrated through the complete width of the test section, not a "cross-section" of the flow field in the model's plane of symmetry.

It was observed that the bent sting produced a strong normal shock wave, which changed the flow around the model, and it is most visible in the snapshots of the Schlieren visualization at Mach 1.5. It was assumed that its occurrence may be influenced by the main balance measurement, as the same level of the drag reduction was not obtained in the force measurement.

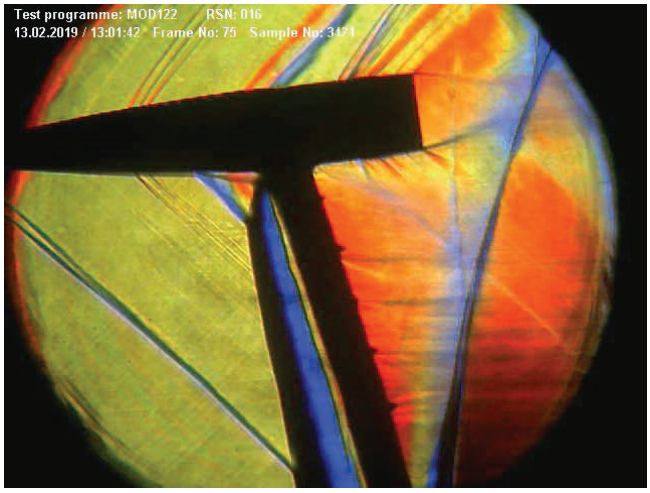

Figure 12. Flow visualization around the model in the Mach 1.5 test

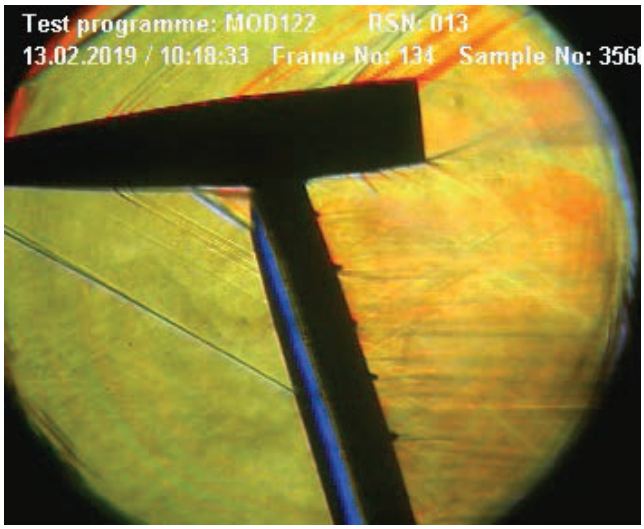

Figure 13. Flow visualization around the model in the Mach 2 test

Conclusion

The experimental simulation of the base-bleed of the combustion products of the gas generator was successfully performed in the T-38 trisonic blowdown wind tunnel and effects of the base-bleed on the aerodynamic characteristics of the axi-symmetric projectile were obtained.

The designer of the projectile emphasized that the hot gas generator has a high influence on the base drag reduction. The use of the real hot gas generator was not possible in the wind tunnel because of safety of the equipment as combustion products are very corrosive. So, the only solution was to design and produce the model of projectile with the gas generator using the high pressure installation.

The base drag reduction that was found in the supersonic tests is about 5% to 8%. The wind tunnel test results were related to the expectations and numerical predictions given by the designer, which are about 11%. Numerical predictions, given by other authors, were about 35% for the supersonic flight stages for this type of projectiles. The obtained drag reduction in the wind tunnel tests were lower than they had numerically been predicted. However, wind tunnel test results were found to be very useful as they showed it is possible to estimate the optimum mass flow rate for minimal drag force in the Mach number range which is coresponding to the real flight stages.

The experimental setup that had to be used because of available equipment constrains (using a cylindrical bent sting for supporting the model from the side) turned out not to be a good design solution. One of the recommendations for future tests is to use a more slender strut blade with a diamond or a rhomboid profile.

During wind tunnel test it was found that a better design solution should be sought for decoupling of the high-pressure pneumatic installation from the live side of the balance. Obtained experience and recommendations are expected to be very useful in the design of future similar wind tunnel models.

Acknowledgment

This study was supported by the Military Technical Institute (VTI) and the Ministry of Education, Science and Technological Development of Serbia (Project number 451-03-9/2021-14/200325).

References

[1] REGODIĆ,D., JEVREMOVIĆ,A., JERKOVIĆ,D.: *The Prediction of Axial Aerodynamic Coefficient Reduction using Base Bleed*, *Aerospace Science and Technology* 31 (2013), pp.24–29.

[2] DAMLJANOVIĆ,D., OCOKOLJIĆ,G., MARINKOVSKI,D., ĐURĐEVAC,D.: *An Experimental Setup for Testing Base-Bleed Configurations of Axisymmetric Projectiles*, Invited Lecture, Proceedings of the 9th International Scientific Conference on Defensive Technologies OTEH 2020, ISBN 978-86-81123-83-6, Belgrade, 15-16, October 2020, pp.2-7.

[3] OCOKOLJIĆ,G., RAŠUO,B., BENGIN,A.: *Aerodynamic Shape Optimization of Guided Missile Based on Wind Tunnel Testing and CFD Simulation*, Thermal Science, Society of Thermal Engineers of Serbia, ISSN: 0354-9836, 2017., 21, 3, pp.1543-1554.

[4] LINIĆ,S., OCOKOLJIĆ,G., RISTIĆ,S., LUČANIN,V., KOZIĆ,M., RAŠUO,B., JEGDIĆ,B.: *Boundary Layer Transition Detection by Thermography and Numerical Method Around Bionic Train Model in Wind Tunnel*, Thermal Science, 10.2298/TSCI170619302L, 2017.

[5] OCOKOLJIĆ,G., ŽIVKOVIĆ,S., SUBOTIĆ,S.: *Aerodynamic Coefficients Determination for the Anti Tank Missile model with Lateral Jets*, Proceedings of the 4th International Scientific Conference on Defensive Technologies, OTEH 2011, Belgrade, 6-7 October 2011.

[6] OCOKOLJIĆ,G., SAMARDŽIĆ,M., Vitić,A.: *Testing of the Anti-Tank Missile Model with Lateral Jets*, Proceedings of the 47th International Symposium of Applied Aerodynamics, Paris, March, 2012

[7] OCOKOLJIĆ,G., RAŠUO,B.: *Testing of the Anti Tank Missile Model with Jets Simulation in the T-35 Subsonic Wind Tunnel*, Scientific Technical Review, Vol.62, No.3-4, 2012., pp.14-20.

[8] AMIN DALI, M., JARAMAZ,S., JERKOVIĆ,D., DJURDJEVAC,D.: *Increasing the Range of Contemporary Artillery Projectiles*, Technical Gazette 26, 4(2019), pp. 960-969, ISSN 1330-3651 (Print), ISSN 1848-6339 (Online), https://doi.org/10.17559/TV-20171219141541.

[9] TRIMMER,L.L., CLARK,E.L.: *Transformation of Axes Systems by Matrix Methods and Application to Wind Tunnel Data Reduction*, NOLR 1241, August 1962

[10] GALWAY,R.D.: *A Comparison of Methods for Calibration and Use of Multi-Component Strain Gauge Balances*, NAE Aeronautical report LR-600, March 1980

[11] STEINLE,F., STANEWSKY,E.: *Wind Tunnel Flow Quality and Data Accuracy Requirements*, AGARD Advisory report No.184, November 1982

[12] ELFSTROM,G.M., MEDVED,B.: *The Yugoslav 1.5m Trisonic Blowdown Wind Tunnel*, Paper 86-0746-CP, AIAA, 1986.

[13] Belaidouni,H., Živković,S., Samardžić, M.: *Numerical Simulations in Obtaining Drag Reduction for Projectile with Base Bleed*, Scientific Technical Review, 2016, Vol.66, No.2, pp.36-42.

[14] VUKOVIĆ,Đ, ILIĆ,B, VITIĆ,A.: *Modernization of the Flow Visualization System in the T-38 Wind Tunnel of Vojnotehnički institut*, in: Proceedings of the 31st Conference on Hydro-pneumatic automation, 2008, Vrnjačka Banja, Serbia, pp. 273-278.

Received: 24.06.2021.
Accepted: 10.11.2021.

Aerotunelska verifikacija efekata isticanja mlaza na aerodinamičke karakteristike osnosimetričnog projektila

Tokom razvoja osnosimetričnog projektila bila je potrebna aerotunelska verifikacija efekata isticanja mlaza na aerodinamičke karakteristike za faze supersoničnog režima leta. Aerotunelska konfiguracija modela projektila sa aktivnim gasogeneratorom u zoni baze za ispitivanje efekata isticanja mlaza je projektovana, izrađena i ispitana u trisoničnom aerotunelu T-38 Vojnotehničkog instituta u Beogradu. Gasogenerator čini jednostavna komora sa jednim piskom pneumatski povezanog na instalaciju visokog pritiska. Aerotunelska ispitivanja su obuhvatala merenje aerodinamičkih sila i momenta sa aktivnim isticanjem mlaza u zoni baze modela. Strujno polje oko modela je vizualizovano šliren metodom. Bilo je od interesa verifikovati smanjenje baznog otpora korišćenjem gasogeneratora u aerotunelskim testovima i uporediti sa numeričkim procenama. Zaključeno je da je iskustvo stečeno tokom ovih ispitivanja izuzetno značajno za projektovanje budućih sličnih eksperimentalnih postavki.

Ključne reči: **aerotunel, projektil, gasogenerator, isticanje mlaza, aerodinamičke karakteristike, bazni otpor.**